Cell – Vessel Mismatch in Glaucoma: Correlation of Ganglion Cell Layer Soma and Capillary Densities

Ricardo Villanueva,[1,2] Christopher Le,[3] Zhuolin Liu,[2] Furu Zhang,[2] Laurence Magder,[4] Daniel X Hammer,[2] and Osamah Saeedi[1]

[1]Department of Ophthalmology and Visual Sciences, University of Maryland School of Medicine, Baltimore, Maryland, United States
[2]Center for Devices and Radiological Health, US Food and Drug Administration, Silver Spring, Maryland, United States
[3]University of Maryland School of Medicine, Baltimore, Maryland, United States
[4]Department of Epidemiology and Biostatistics, University of Maryland School of Medicine, Baltimore, Maryland, United States

Correspondence: Osamah Saeedi, Department of Ophthalmology and Visual Sciences, University of Maryland School of Medicine, 655 West Baltimore Street, Baltimore, MD 21201, USA; osaeedi@som.umaryland.edu.

RV and CL contributed equally to this publication and should be considered co-first authors.

Received: May 17, 2021
Accepted: August 27, 2021
Published: October 4, 2021

Citation: Villanueva R, Le C, Liu Z, et al. Cell – vessel mismatch in glaucoma: Correlation of ganglion cell layer soma and capillary densities. *Invest Ophthalmol Vis Sci.* 2021;62(13):2. https://doi.org/10.1167/iovs.62.13.2

Purpose. The purpose of this study was to characterize the relationship between retinal ganglion cell layer (GCL) soma density and capillary density in glaucomatous eyes.

Methods. Six glaucoma subjects with known hemifield defects and 6 age-matched controls were imaged with adaptive optics – optical coherence tomography (AO-OCT) at 6 locations: 3 degrees, 6 degrees, and 12 degrees temporal to the fovea above and below the midline. GCL soma density and capillary density were measured at each location. Coefficients of determination (pseudo R^2) and slopes between GCL soma and capillary density were determined from mixed-effects regressions and were compared between glaucoma and control subjects, between more and less affected hemifield in subjects with glaucoma, and between subjects with early and moderate glaucoma, both in a local, bivariate model and then a global, multivariable model controlling for eccentricity and soma size.

Results. The global correlation between GCL soma and capillary density was stronger in control versus subjects with glaucoma ($R^2 = 0.59$ vs. 0.22), less versus more affected hemifields ($R^2 = 0.55$ vs. 0.01), and subjects with early versus moderate glaucoma subjects ($R^2 = 0.44$ vs. 0.18). When controlling for eccentricity and soma size, we noted an inverse soma-capillary density local relationship in subjects with glaucoma (-388 ± 190 cells/mm^2 per 1% change in capillary density, $P = 0.046$) and more affected hemifields (-602 ± 257 cells/mm^2 per 1% change in capillary density, $P = 0.03$).

Conclusions. An inverted soma-capillary density local relationship in areas affected by glaucoma potentially explains weaker global correlations observed between GCL soma and capillary density, suggesting cell–vessel mismatch is associated with the disease.

Keywords: glaucoma, adaptive optics, structure-structure, capillary density, soma density

Glaucoma is a leading cause of irreversible blindness worldwide[1] and its only current treatment is reduction of intraocular pressure (IOP). However, glaucoma can worsen in up to 45% of patients with early glaucoma despite therapeutic reduction in IOP,[2] and up to one-third of patients develop glaucoma with IOP in the normal range, indicating that non-IOP related factors contribute to the disease. Whereas retinal ganglion cells (RGCs) and their axons are the primary site of glaucomatous damage, strong evidence also implicates retinal vascular dysfunction in the disease.[3–5] In all stages of glaucoma, changes in retinal vascular structure (e.g. vessel dropout) are present.[6] In order to develop novel treatment strategies that target both the cellular and vascular component of glaucoma, precise benchmark measurements of the interaction between RGCs and their vascular supply must be established.

Current vascular structural data show that glaucomatous damage is associated with decreased superficial macular vessel density as measured by optical coherence tomography angiography (OCT-A).[7] Ganglion cell-inner plexiform layer (GC-IPL) thickness, while informative, is a surrogate for RGC density, and direct measures of RGC density may permit a more accurate assessment of effects at the scale of a neurovascular unit.

Until recently, quantification of RGC density was limited to ganglion cell layer (GCL) thickness measurement with optical coherence tomography (OCT). By pairing adaptive optics (AO) technology with scanning laser ophthalmoscopy (AO-SLO) and OCT (AO-OCT), it is now possible to obtain three-dimensional, cellular-level structural images of the optic nerve head and retina to study glaucoma.[8–17] Newly demonstrated AO-OCT methods can reliably quantify GCL soma morphology and density[17–20] and can distinguish retinal capillaries[21] at significantly higher resolution than commercially available OCT-A, enabling analysis at multiple eccentricities from the fovea within the macula.

Importantly, AO-OCT can isolate the density of vessels and vascular plexuses[22] that specifically nourish RGCs.[23]

In the macula, retinal vessels separate into three distinct vascular plexuses away from the foveal avascular zone: the superficial vascular plexus (SVP), intermediate capillary plexus (ICP), and deep capillary plexus (DCP). The SVP resides in the GCL and primarily nourishes RGCs and their axons that make up the retinal nerve fiber layer (RNFL). The ICP is at the base of the inner plexiform layer (IPL) and supplies the dendritic synapses in that layer as well as the cells in the inner nuclear layer (INL). The DCP is at the base of the INL and mainly supplies the bipolar and horizontal cells and their connections to the photoreceptor outer nuclear layer.

The purpose of the current study is to determine the global and local relationship between vascular and GCL soma densities in healthy and glaucoma subjects. We take advantage of high-resolution, precise optical sectioning and subcellular accuracy registration of AO-OCT to simultaneously image retinal vessels and GCL soma densities at multiple eccentricities across the macula. This method allows for a detailed investigation of the relationship between the two, ultimately linking two key structural metrics of the inner retina important in glaucoma pathophysiology. We have previously shown that GCL soma density is significantly lower in eyes with glaucoma compared to age-matched control subjects across the macula.[17] We hypothesize that in healthy control subjects higher cell density requires increased perfusion for metabolism and these locations will therefore require greater vascular supply and have higher capillary density. We further hypothesize that, in subjects with glaucoma, disruption of local cellular perfusion results in a mismatch between vascular supply and RGC density, manifest as an altered relationship between GCL soma density and capillary density.

Materials and Methods

This paper uses AO-OCT data collected from a cohort of subjects with glaucoma and control subjects previously analyzed in a study centered around GCL soma morphology quantification.[17] The full details of subject clinical assessment, AO imaging, and GCL soma analysis are found in a previously published paper,[17] aspects of which are summarized below. The current study extends the previous GCL soma density results with analysis of the density of vascular plexuses that supply the GCL cells. As previously, in this paper, we use the term GCL soma rather than RGC soma because we do not distinguish between RGCs and the small proportion of displaced amacrine cells that make up the GCL.

Study Population and Clinical Assessment

This research protocol was approved by the Institutional Review Boards of the US Food and Drug Administration (FDA) and the University of Maryland and adhered to the tenets of the Declaration of Helsinki. Written informed consent was obtained after the potential risks were explained to each participant. All subjects were evaluated by an experienced glaucoma specialist (author O.J.S.) and underwent gonioscopy, dilated fundus examination, and spectral domain-optical coherence tomography (SD-OCT). In addition to those tests, subjects with glaucoma had standard automated perimetry (SAP) with Humphrey visual field (HVF). Subjects with glaucoma were diagnosed with primary open angle glaucoma (POAG) based on American Academy of Ophthalmology Practice Patterns.[24] Glaucoma severity was designated as early, moderate, or severe based on Hodapp-Anderson-Parrish criteria as applied to the most recent visual field.[25] We purposely recruited subjects with glaucoma with asymmetric glaucomatous damage across the horizontal midline with relatively more RNFL and GCL thinning on one side of the hemifield that corresponded to visual field loss on the opposite side of the damaged RNFL and GCL area in order to compare soma and capillary density between the more and less affected hemifields within the same patient. Control subjects had an OCT RNFL within normal limits in all quadrants, IOP below 21 mm Hg, symmetric and healthy neuroretinal rims, and a cup-to-disc ratio of 0.5 or less.

In Vivo AO Imaging

GCL Soma Density and Size Quantification. Pupillary dilation and cycloplegia was achieved with 1% tropicamide in subjects, who were subsequently imaged using the FDA multimodal adaptive optics (mAOs) device previously described.[17,26] We examined six 1.5 degrees × 1.5 degrees regions located symmetrically 2.5 degrees superior (S) and inferior (I) about the horizontal midline at eccentricities 3 degrees, 6 degrees, and 12 degrees in the temporal (T) retina (Fig. 1A). These eccentricities were selected to observe glaucoma-associated regional differences. The AO focus was set to the GCL and 300 AO-OCT volumes were collected, registered, and averaged at each location. GCL soma centers across the full layer depth were manually counted from each averaged volume with custom cell counting software in MATLAB (Fig. 1C). Of 72 total locations from the 12 subjects, 6 volumes were insufficient quality for soma quantification and were excluded from analysis. Image quality metrics were not available and the determination of adequacy of image quality was determined by the grader (author R.V.). Image quality was qualitatively similar between disease groups. GCL soma density was calculated by projecting the soma counts onto a single en face plane. A Voronoi map, a mathematical construct widely used to quantify retinal cells,[27] was then applied to the en face image, and density was determined by calculating the ratio between the number of Voronoi cells and the total area occupied by the Voronoi cells, after excluding any region occupied by blood vessels. The diameter of each soma was computed through a similar projection onto a single en face plane followed by superimposition of a generated radial profile from the soma center. The soma diameter was defined as twice the length of the minimum radial profile within the region of interest determined from this superimposition. The average soma size was calculated from all soma within an imaged location. Soma sizes across eccentricity and disease state are summarized in Supplementary Table S1. These diameter values were used in our mixed-effects modeling to account for the effects of soma size on the local GCL soma-capillary relationship.

Capillary Density Calculation. In the same AO-OCT volumes, the SVP and ICP, the two retinal vascular plexuses that supply the GCL somas and their dendrites, were segmented by first reviewing each volume and vessels within each plexus, then selecting the relevant slices for each plexus, and finally creating an en face average

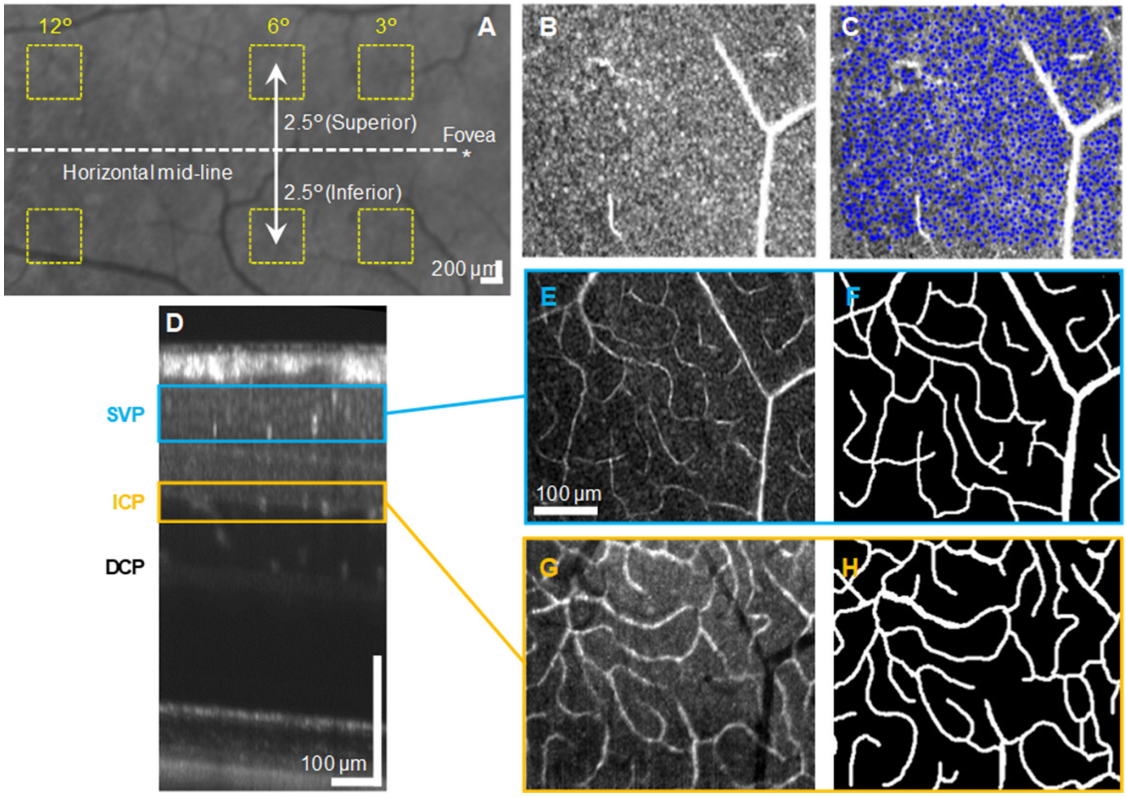

Figure 1. AO-OCT methods for GCL soma and capillary (SVP and ICP) density measurement. (**A**) Six AO-OCT locations imaged in the temporal macula with respect to the horizontal mid-line and fovea. (**B, C**) En face AO-OCT images of GCL of single plane at 3T2.5I in one healthy control subject with and without GCL somas marked (*blue crosses*). (**D**) AO-OCT B-scan demonstrating relative locations of the SVP, ICP, and DCP. En face AO-OCT projection and corresponding binarized vessel map of (**E, F**) the SVP and (**G, H**) the ICP.

intensity projection across the axial pixels in which each plexus resides (Fig. 1D).[28] All vessels clearly distinguishable in each en face projection were then manually traced by a single grader (author R.V.) using a uniform brush size for each capillary segment. For each capillary branch, the brush size was readjusted depending on the grader's visual estimate of that segment's vessel width. These tracings were binarized in ImageJ (Fig. 1F).[29] The grader was not explicitly masked to the disease state. Capillary density was defined as the fractional capillary area, or the percentage of pixels in each 1.5 degrees × 1.5 degrees field-of-view occupied by vessels less than 20 µm in diameter. This diameter threshold was selected to limit the analysis to capillaries, which typically range from 5 to 15 µm in diameter, and reduce the inclusion of arterioles and venuoles, which are 30 µm in diameter on average.[30–32]

SVP and ICP capillary densities were summed to measure the overall capillary contribution to GCL soma metabolism, which we call the GC-IPL capillary density. Figure 1 shows representative en face GCL soma and vascular images from one healthy control subject at 3°T, as well as the binary vessel maps generated from manual tracings.

Statistical Analysis

We assessed densities of GCL soma and GC-IPL capillaries at each eccentricity and compared these values for 3 cases: (1) between glaucoma and control subjects, (2) between more and less affected hemifields in subjects with glaucoma, and (3) between subjects with early and moderate glaucoma. All comparisons accounted for repeated measures and were assessed with a *t*-test using Satterthwaite's approximation with $P < 0.05$ values considered significant. To assess an overall relationship across the macula between soma and capillary density, we fit linear mixed-effects regression models between GCL capillary density and GC-IPL soma density, pooling across eccentricity, stratified for each comparison. These bivariate models do not account for eccentricity and provides an estimate of the global relationship between soma and capillary density. As we utilized linear mixed-effects models to account for within-patient variance in repeated measures, we calculated a marginal pseudo R^2 as a coefficient of determination to quantify how well capillary density explains the variation in soma density.[33] Because it was clear from our original GCL soma quantification study[17] that soma densities are highly dependent on eccentricity, further statistical analysis was performed to distinguish among factors that may contribute to the local correlation. Therefore, we also subsequently fit multivariable linear mixed-effects models to assess the relationships between GCL soma density and GC-IPL capillary density while accounting for the fixed effects of disease state, eccentricity, average soma size, and GC-IPL capillary density. These multivariate models account for the effects of eccentricity and provide an estimate of the local relationship between soma and capillary density. In all models, we included a random effect at the patient level to account for the repeated observations from the same person. We used SAS version 9.4 (SAS Institute, Cary, NC, USA) and R version 4.0.5 (R Foundation, Vienna, Austria) for statistical analysis.

Investigative Ophthalmology & Visual Science

Table 1. Subject Demographics

	Glaucoma ($n = 6$)	Control ($n = 6$)
Age (y)	58.1 ± 4.5	61.1 ± 8.3
Race		
White	3 (50%)	5 (83.3%)
Non-White	3 (50%)	1 (16.7%)
Sex		
M	1 (16.7%)	6 (100%)
F	5 (83.3%)	0 (0%)
Axial length (mm)	23.8 ± 1.2	24.4 ± 1.4
Peripapillary RNFL thickness (µm)	89.3 ± 11.3	92.7 ± 6.5
Glaucoma severity		
Early	3 (50%)	
Moderate	3 (50%)	
Visual Field Index 24-2 (%)	91 ± 0.06	
Mean deviation 24-2 (dB)	−2.7 ± 2.8	
Pattern standard deviation 24-2 (dB)	3.7 ± 1.1	

Results

Our sample included six subjects with glaucoma and six age-matched control subjects. Demographics of each cohort are described in Table 1.

Global Relationship Between GCL Soma and GC-IPL Capillary Density

We first examined the global relationship between GCL soma density and GC-IPL capillary density in all 12 subjects (Fig. 2). Among the six control subjects, the average GCL soma density decreases across the macula from 4 to 5 cell layers deep at 3°T (25,058 ± 4649 cells/mm^2), to 2 to 3 layers at 6°T (15,551 ± 2301 cells/mm^2), to a monolayer at 12°T (3891 ± 1105 cells/mm^2; see Fig. 2A).[17] Subjects with glaucoma followed the same trend but had lower GCL soma density than control subjects across all three locations: 3°T (12,799 ± 7747 cells/mm^2), 6°T (9370 ± 5572), and 12°T (2134 ± 1494; see Fig. 2A). The difference between mean control and glaucoma GCL density was significant at each eccentricity (P value < 0.05). The GC-IPL capillary density also decreased as a function of eccentricity in a similar trend among subjects with glaucoma and control subjects (Fig. 2B). The capillary density was 0.27 ± 0.03 (3°T), 0.22 ± 0.03 (6°T), and 0.19 ± 0.03 (12°T) for subjects with glaucoma and 0.30 ± 0.04 (3°T), 0.26 ± 0.04 (6°T), and 0.18 ± 0.03 (12°T) for control subjects. The difference between mean control and glaucoma GC-IPL capillary density was not significant at any eccentricity (P value = 0.10, 0.06, and 0.89). Figure 2C shows the global relationship between GCL soma density and GC-IPL capillary density in control subjects and subjects with glaucoma not accounting for eccentricity or soma size. The coefficient of determination was relatively high for control subjects (pseudo $R^2 = 0.59$) and much lower for subjects with glaucoma (pseudo $R^2 = 0.22$).

Within the subjects with glaucoma, we compared the GCL soma and GC-IPL capillary density values between more and less affected hemifields. Among the less affected hemifield of the glaucomatous eyes (i.e. the healthier side), the average GCL soma density values were 17,406 ± 3763 (3°T), 13,621 ± 2520 (6°T), and 2769 ± 1095 (12°T; Fig. 3A). In the more affected hemifields, the average GCL soma density values were 8959 ± 8111 (3°T), 4507 ± 4400 (6°T), and 1372 ± 1551 (12°T). Across the macula, compared to the less affected hemifield, the more affected hemifield had lower GCL density. These differences in mean GCL density between more and less affected hemifield were not significant at 3 degrees and 12 degrees but was significant at 6 degrees (P value = 0.08, 0.01, and 0.16). We observed slightly lower average GC-IPL capillary densities at all eccentricities in the more affected hemifield: 0.27 ± 0.03 (3°T), 0.20 ± 0.03 (6°T), and 0.16 ± 0.03 (12°T), compared to the less affected hemifield: 0.27 ± 0.02 (3°T), 0.24 ± 0.02 (6°T), 0.20 ± 0.02 (12°T; Fig. 3B). These differences in mean capillary density between more and less affected hemifield were

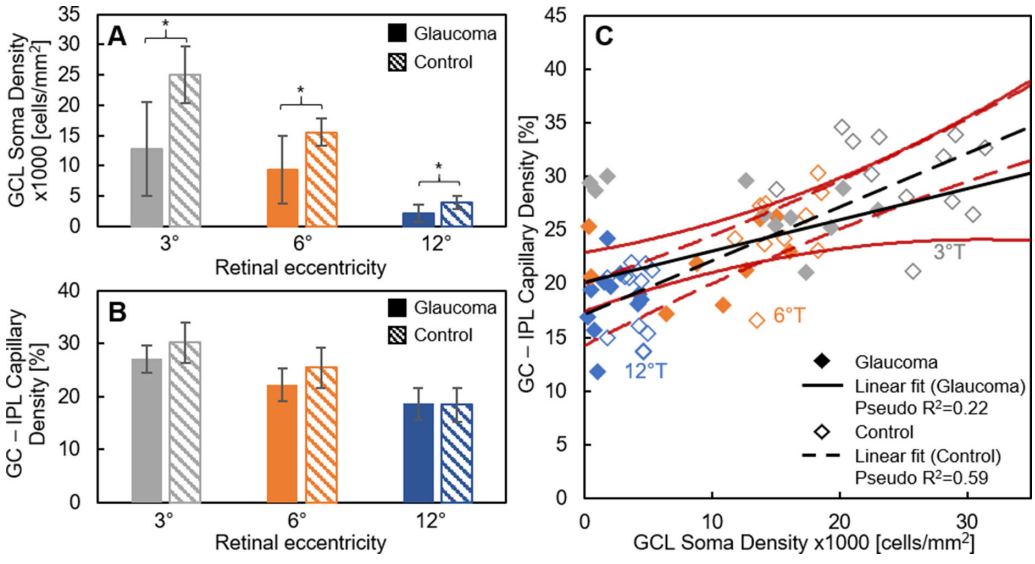

Figure 2. A comparison of GCL soma density and GC-IPL capillary density between control and subjects with glaucoma at 3°T, 6°T, and 12°T. (**A**) The mean GCL soma density for glaucoma and control subjects at all three locations. (**B**) Average GC-IPL capillary density at each location. The error bars represent standard deviation. (**C**) The relationship between GC-IPL capillary density and GCL soma density is fit by a slope from our bivariate mixed-effects regression (red lines indicate 95% confidence intervals for glaucoma [*solid*] and control [*dashed*], respectively). Open and filled symbols represent control and glaucoma subjects, respectively (* P value < 0.05).

Investigative Ophthalmology & Visual Science

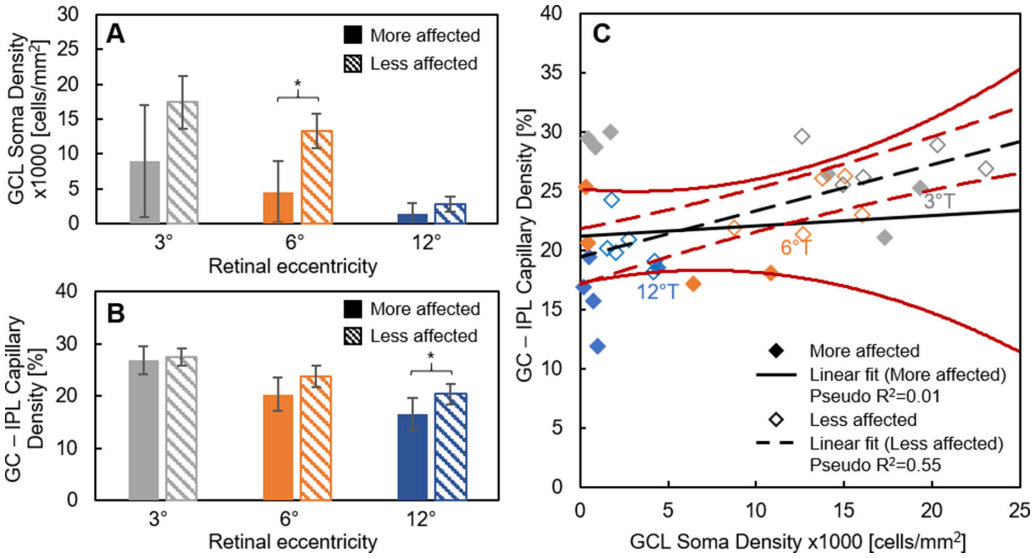

Figure 3. The relationship between GC-IPL capillary and GCL soma density in glaucoma hemifield locations. (**A**) Average GCL soma density at each location for more and less affected hemifield location. (**B**) Average GC-IPL capillary density at each location. The error bars represent standard deviation. (**C**) The relationship between GC-IPL capillary density and GCL soma density for hemifield locations is fit by a slope from our bivariate mixed-effects regression (red lines indicate 95% confidence intervals; * P value < 0.05).

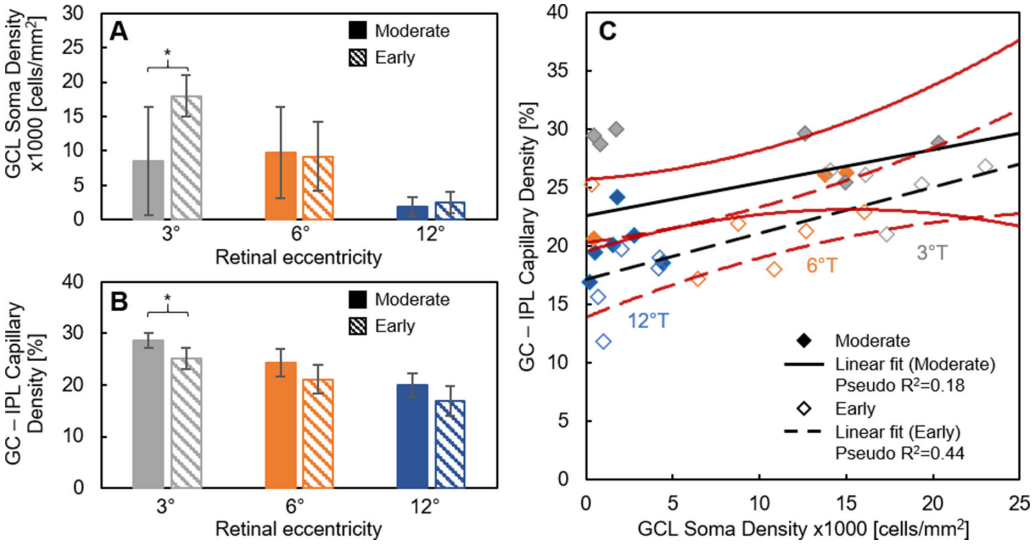

Figure 4. The relationship between GCL soma and GC-IPL capillary density in subjects with early and moderate glaucoma. (**A**) Average GCL soma density values for the three eccentricities. (**B**) Average GC-IPL capillary density values for the three eccentricities. The error bars represent standard deviation. (**C**) The relationship between GC-IPL capillary density and GCL soma density for subjects with early and moderate glaucoma is fit by a slope from our bivariate mixed-effects regression (*red lines* indicate 95% confidence intervals, *P value < 0.05).

not significant at 3 degrees and 6 degrees but was significant at 12 degrees (P value = 0.69, 0.14, and 0.01). Less affected hemifields have a stronger coefficient of determination (pseudo R^2 = 0.55) compared to the more affected hemifield (pseudo R^2 = 0.01; Fig. 3C) in the bivariate regression between soma and capillary density not accounting for eccentricity or soma size. In fact, the coefficient of determination of the less affected hemisphere (pseudo R^2 = 0.55) is comparable to that of the control subjects (pseudo R^2 = 0.59).

We assessed the GCL soma and GC-IPL capillary density values in subjects with early and moderate glaucoma. The GCL soma density is higher at the 3 degrees and 12 degrees locations in subjects with early glaucoma: 17,983 ± 3048 (3°T) and 2446 ± 1518 (12°T) compared with subjects with moderate glaucoma: 8478 ± 7824 (3°T) and 1875 ± 1423 (12°T; Fig. 4A). At the 6 degree location, the soma density was higher in subjects with moderate glaucoma (9760 ± 6602) than subjects with early glaucoma (9175 ± 4966). These differences in mean GCL density between early and

Table 2. Soma – Capillary Density Regression Coefficients from Multivariable Mixed-Effects Models

	Soma – Capillary Density Regression Coefficient [Cells/mm^2 Per 1% Change in Capillary Density] [95% Confidence Interval]	*P* Value for Difference in Soma-Capillary Density Regression Coefficient Between Compared Groups
Control versus glaucoma		
Control subjects	220 [−92 to 532]	0.03*
Glaucoma subjects*	−388 [−760 to −16]	
Less versus more affected Hemifield		
Less affected Hemifield	−67 [−579 to 445]	0.05
More affected Hemifield*	−602 [−1106 to −98]	
Early versus moderate glaucoma		
Early glaucoma subjects	465 [−270 to 1200]	0.20
Moderate glaucoma subjects	−107 [−671 to 457]	

* *P* value < 0.05.

moderate glaucoma was significant at 3 degrees, but not at 6 degrees or 12 degrees (*P* value = 0.04, 0.90, and 0.59).

Conversely, the GC-IPL capillary density is lower in subjects with early glaucoma: 0.25 ± 0.02 (3°T), 0.21 ± 0.03 (6°T), and 0.17 ± 0.03 (12°T) compared with subjects with moderate glaucoma: 0.29 ± 0.01 (3°T), 0.24 ± 0.03 (6°T), and 0.20 ± 0.02 (12°T; Fig. 4B). The differences in capillary density between early and moderate glaucoma was significant at 3 degrees, but not at 6 degrees or 12 degrees (*P* value = 0.04, 0.25, and 0.10; Fig. 4C). Subjects with early glaucoma also had a stronger coefficient of determination (pseudo R^2 = 0.44) compared with subjects with moderate glaucoma (pseudo R^2 = 0.18) in the bivariate regression between soma and capillary density not accounting for eccentricity or soma size.

Local Relationship Between GCL Soma Density and GC-IPL Capillary Density

Table 2 summarizes the results of the multivariable mixed model analysis for the 3 cases considered in this paper. The mixed model regression coefficient represents the slope of the relationship between GCL soma and capillary densities while controlling for local measured factors (eccentricity, etc.) expressed in units of cell density (cells/ mm^2) per 1% change in capillary density.

The relationships in Figures 2C, 3C, and 4C were due, in part, to the fact that both GCL soma density and GC-IPL decreased with eccentricity. Our mixed-effects model controlling for eccentricity and average soma size, found that in control subjects, the correlation between GCL soma density and GC-IPL capillary density was not significant and positive (regression coefficient [95% confidence interval] = 220 [95% confidence interval −92, 532] cells/mm^2 per 1% change in capillary density, *P* value = 0.17), whereas in subjects with glaucoma, the soma-vessel relationship was significant and negatively correlated (−388 [95% confidence interval −760, −16] cells/mm^2 per 1% change in capillary density, *P* value = 0.046). The difference between the soma-vessel relationship in subjects with glaucoma and control subjects was significantly different (*P* value = 0.03; see Table 2).

Our multivariable mixed-effects model found that in less affected hemifields, the soma-vessel relationship was nonsignificant and negatively correlated (−67 [95% confidence interval −579, 445] cells/mm^2 per 1% change in capillary density, *P* value = 0.8), whereas in more affected hemifields, the soma-vessel relationship was significant and negatively correlated (−602 [95% confidence interval −1106, −98] cells/mm^2 per 1% change in capillary density, *P* value = 0.03). The difference between the soma-vessel relationship in more and less affected hemifields was not significantly different (*P* value = 0.05; see Table 2).

Our multivariable mixed-effects model found that in early glaucoma, the soma-vessel relationship was nonsignificant and positive (465 [95% confidence interval −270, 1200] cells/mm^2 per 1% change in capillary density, *P* value = 0.23), whereas in moderate glaucoma subjects, the soma-vessel relationship was nonsignificant and negatively correlated (−107 [95% confidence interval −671, 457] cells/mm^2 per 1% change in capillary density, *P* value = 0.72). The difference between the soma-vessel relationship in early and moderate glaucoma subjects was not significantly different (*P* value = 0.20; see Table 2).

Discussion

Our study is the first to assess the relationship between GC-IPL capillary density and GCL soma density in glaucomatous eyes. Our results show that, globally, these two variables are strongly correlated in control subjects and weaker in subjects with glaucoma, specifically in hemifields more affected by glaucoma, and with more advanced progression, indicating possible impaired cellular perfusion in the disease. We observed a similar or stronger global relationship between GCL soma density and GC-IPL capillary density than has been previously shown with retinal layer thickness and capillary density using standard clinical OCT and OCT-A. However, when we account for the effect of eccentricity and soma size in our multivariable model reflecting the local relationship between soma and capillary density, we also find that the globally weaker relationship in subjects with glaucoma is significant and negative when accounting for the local effects of eccentricity and soma size. These findings in the global and local correlation between soma and capillary density have important implications about the relationship between neurons and their vascular supply in healthy states and neurodegenerative diseases, such as glaucoma.

Previous studies have explored the associations between retinal structural measures and vascular parameters in subjects with and without glaucoma.[7,34,35] However, these studies used clinical SD-OCT and therefore relied on coarser retinal layer thickness measurements as a surrogate quantification of retinal cell density and circularly defined sectors around the foveal avascular zone (FAZ) larger than 1 mm^2 to define focal effects. AO-OCT allows for a more detailed

Investigative Ophthalmology & Visual Science

assessment of the relationship between structural and vascular parameters, which accounts for eccentricity and soma diameter. Additionally, these studies reported the association between vessels and layer thickness solely within glaucomatous eyes, and do not report coefficient of determinations within control subject eyes for comparison. Richter et al. studied the association between macular GC-IPL thickness and microvascular parameters within the same layer in 23 subjects with POAG and 16 control subjects and found a significant association between inferior GC-IPL thickness and vessel area density with a pseudo R^2 of 0.16.[7] Our results in our analogous regression analysis that does not account for eccentricity or soma diameter show a significant global association for subjects with glaucoma with a similar coefficient of determination (pseudo $R^2 = 0.22$).

Kim et al. found a significant association between superotemporal (ST), inferotemporal (IT), and inferoinferior (II) macular thickness in 25 eyes from subjects with glaucoma and 86 eyes from subjects with early-stage normal tension glaucoma.[34] They attributed the more significant associations in more regions compared to Richter et al. in part to their choice to exclude large vessels, which we also excluded from our analysis. Although we did not specifically evaluate early normal tension in subjects with glaucoma or glaucoma suspects, previous studies have demonstrated similar vascular and retinal layer thickness changes in normal tension glaucoma and early primary open angle glaucoma.[36,37] Kim et al. found coefficient of determinations for the associations in the ST, IT, and II regions ($R^2 = 0.037$, 0.14, and = 0.12, respectively). The strong association in early glaucoma subjects within our study (pseudo $R^2 = 0.44$) may reflect the intrinsic advantages of cellular density measurement by AO-OCT compared to layer thickness measurement with standard OCT imaging.

Takusagawa et al. studied the association between the ganglion cell complex (GCC) thickness and the superficial vascular plexus combined with radial peripapillary capillary plexus as the superficial vascular complex (SVC) for 30 subjects with perimetric glaucoma and 30 age-matched control subjects.[35] Augmenting standard OCT with projection-resolved OCT-A algorithms that improve capillary detection in deeper layers and implementing reflectance adjustment algorithms, they found significant associations between GCC thickness and SVC vessel density ($R^2 = 0.65$) as well as a significant but weaker association between GCC thickness and all-plexus vessel density ($R^2 = 0.19$) within their subjects with glaucoma. The stronger associations found by Takusagawa et al. are attributed to the use of post-processing algorithms that alleviate, but do not fully remove, projection artifacts (tails) and local noise found in conventional OCT-A. Although the results of Takusagawa et al. demonstrate a stronger correlation between vessel density and layer thickness within glaucomatous eyes, they do not compare these values to control subjects or compare the more affected to the less affected hemifield.

When controlling for eccentricity and average soma size with a multivariable mixed effect model, we observed a significant negative correlation between soma density and capillary density in subjects with glaucoma, indicating that GCL soma density decreases with increased capillary density. This correlation significantly differs between subjects with glaucoma and control subjects. Although soma and capillary density appear positively correlated in subjects with glaucoma in all previously discussed studies and our global, bivariate models where the effect of eccentricity and average soma size is unaccounted for, they are significantly negatively correlated locally (i.e. when the effects of eccentricity and soma size are considered). The same trend is observed when we compare hemifields in subjects with glaucoma where both hemifields have a negative correlation, but the local relationship is stronger and significant in the more affected hemifield. The negative correlation in subjects with glaucoma corresponds with a lower pseudo R^2 in the global relationship between capillary and soma densities in glaucoma subjects in our bivariate regression analysis, suggesting that cell–vessel mismatch in glaucoma is not simply greater global variation among the soma-capillary density relationships, but rather a specific inversion of the localized relationship between RGCs and vasculature. That is, whereas the strong positive soma-capillary relationship (more cells are matched with more blood supply) seen globally in control subjects appears to be accounted for by eccentricity and/or soma size differences, subjects with glaucoma with weaker global positive relationship can be explained by the opposite relationship locally (less cells are matched with more blood supply). This inverted relationship in glaucoma differs significantly from the local relationship in control subjects. One possible explanation for this seemingly paradoxical inverted local relationship lies in our finding that the average soma diameter in patients with glaucoma is larger than in control subjects.[17] It is possible that cell enlargement in glaucoma could decrease GCL density while still requiring sufficient vessel density to supply the cell. However, our model accounts for average soma size and the negative soma-capillary correlation is significant in glaucoma. This would suggest that differences in soma size alone do not explain the negative local correlation, and that these larger somas may indicate other cellular changes, such as structural damage and fragmentation, that could require more maintenance and vascular support. An alternative explanation is that capillaries in the glaucomatous eye have a dysfunctional autoregulatory capacity or other functional failure despite maintaining a vessel density similar to healthy eyes relative to differences in soma density.[38] Either explanation is consistent with our hypothesis that local cellular perfusion is disrupted in glaucoma, although the timing and mechanism is unclear. For example, one potential mechanism is that impaired ocular perfusion or autoregulation of blood flow predisposes or is causative of glaucomatous cellular changes, whereas another is that the local capillary loss follows cellular damage after some time lag or is limited by a floor effect. Future longitudinal studies will be needed to determine the underlying mechanism behind disrupted cell – vessel spatial relationship in subjects with glaucoma, and whether this altered relationship is indicative of impaired neurovascular coupling.

In the multivariable models, we also observed nonsignificant local soma-capillary density coefficients in control subjects. This finding contrasts with significant global correlations seen in our bivariate analysis when not accounting for eccentricity and soma size. One possible explanation is that our sample size is not adequate to detect a significant local relationship between GCL soma and GC-IPL capillary density in control subjects. However, local heterogeneity in capillary networks has been observed in healthy rat retinal models and hypothesized to be an important feature in the regulation of retinal microcirculation, which is consistent with the lack of significant relationship observed in local models accounting for eccentricity.[39] If this nonsignificant relationship is supported by future studies with larger

Investigative Ophthalmology & Visual Science

samples of healthy, control eyes, the complimentary results of our local and global models would suggest that the stronger spatial correspondence between cell and vessel density in healthy control eyes may be largely driven by factors related to eccentricity and soma size.

Other optic neuropathies, particularly those associated with pituitary adenoma, have manifest both decreased GCC thickness as well as decreased superficial vascular complex density.[40] In this pathologic state, the coefficient of determination between GCC and SVC density parafoveally was also low ($R^2 = 0.06$). Indeed, the loss of neurovascular coupling is implicated in multiple neurodegenerative diseases, including Alzheimer's disease, and so this study and others may serve as models for further study of the role of soma – capillary density correlation in neurodegenerative disease.[41]

Limitations of this work include a relatively limited sample size. When comparing the demographic differences between glaucoma and control groups there is some possibility of confounding influence as the subjects with glaucoma group has a greater proportion of women and non-White subjects. These differences may be accounted for in future, larger sample size studies with a more balanced proportion of these groups. Further, given the limited sample size, we cannot rule out the possibility that other relationships, particularly comparisons made between early and moderate glaucoma that are not significant in this study, are revealed to be significant in a larger study. This sample size limitation is also reflected in the limited range of soma and capillary densities seen in our data, which may influence the ability to compare linear fits between these two variables. Larger studies will be needed before extrapolating these results to a larger range of vessel and capillary densities. Additionally, all subjects underwent clinical SD-OCT but did not all have reliable OCT-A scans, limiting the ability to compare our results with OCT-A.

In conclusion, our study shows that areas of high GCL soma density appear to have greater metabolic demand that can be quantified with capillary density measurements within control subjects. Additionally, we show that subjects with glaucoma have a significantly weaker global relationship between GCL soma density and GC-IPL capillary density than control subjects and locally this relationship is significantly negative. This study provides valuable information about the relationship between vascular supply and RGCs and advances our understanding of vessel density as a surrogate biomarker for glaucoma and other optic neuropathies.

Acknowledgments

The authors thank Anant Agrawal for reviewing the manuscript. We also thank Donald Miller (Indiana University School of Optometry) for use of the OCT 3-D registration software.

Supported by a grant from the FDA Critical Path Initiative and the intramural research program of the National Institutes of Health, National Eye Institute and an NIH Career Development Award (K23EY025014) (O.S.).

Disclaimer: The mention of commercial products, their sources, or their use in connection with material reported herein is not to be construed as either an actual or implied endorsement of such products by the US Department of Health and Human Services.

Disclosure: **R. Villanueva**, None; **C. Le**, None; **Z. Liu**, adaptive optics–optical coherence tomography technology (P); **F. Zhang**, adaptive optics–optical coherence tomography technology (P); **L. Magder**, None; **D.X. Hammer**, None; **O. Saeedi**, Heidelberg Engineering (F)

References

1. Flaxman SR, Bourne RRA, Resnikoff S, et al. Global causes of blindness and distance vision impairment 1990-2020: a systematic review and meta-analysis. *Lancet Glob Health*. 2017;5(12):e1221–e1234.
2. Leske MC, Heijl A, Hussein M, et al. Factors for glaucoma progression and the effect of treatment: the early manifest glaucoma trial. *Arch Ophthalmol*. 2003;121(1):48–56.
3. Weinreb RN, Aung T, Medeiros FA. The pathophysiology and treatment of glaucoma: a review. *JAMA*. 2014;311(18):1901–1911.
4. Flammer J, Orgül S, Costa VP, et al. The impact of ocular blood flow in glaucoma. *Prog Retin Eye Res*. 2002;21(4):359–393.
5. Chan KKW, Tang F, Tham CCY, Young AL, Cheung CY. Retinal vasculature in glaucoma: a review. *BMJ Open Ophthalmol*. 2017;1(1):e000032.
6. Wareham LK, Calkins DJ. The Neurovascular Unit in Glaucomatous Neurodegeneration. *Front Cell Dev Biol*. 2020;8:452.
7. Richter GM, Madi I, Chu Z, et al. Structural and Functional Associations of Macular Microcirculation in the Ganglion Cell-Inner Plexiform Layer in Glaucoma Using Optical Coherence Tomography Angiography. *J Glaucoma*. 2018;27(3):281–290.
8. Nadler Z, Wang B, Wollstein G, et al. Repeatability of in vivo 3D lamina cribrosa microarchitecture using adaptive optics spectral domain optical coherence tomography. *Biomed Opt Express*. 2014;5(4):1114–1123.
9. Akagi T, Hangai M, Takayama K, Nonaka A, Ooto S, Yoshimura N. In vivo imaging of lamina cribrosa pores by adaptive optics scanning laser ophthalmoscopy. *Invest Ophthalmol Vis Sci*. 2012;53(7):4111–4119.
10. Hood DC, Lee D, Jarukasetphon R, et al. Progression of Local Glaucomatous Damage Near Fixation as Seen with Adaptive Optics Imaging. *Transl Vis Sci Technol*. 2017;6(4):6.
11. Takayama K, Ooto S, Hangai M, et al. High-resolution imaging of retinal nerve fiber bundles in glaucoma using adaptive optics scanning laser ophthalmoscopy. *Am J Ophthalmol*. 2013;155(5):870–881.
12. Chen MF, Chui TYP, Alhadeff P, et al. Adaptive optics imaging of healthy and abnormal regions of retinal nerve fiber bundles of patients with glaucoma. *Invest Ophthalmol Vis Sci*. 2015;56(1):674–681.
13. Huang G, Luo T, Gast TJ, Burns SA, Malinovsky VE, Swanson WH. Imaging Glaucomatous Damage Across the Temporal Raphe. *Invest Ophthalmol Vis Sci*. 2015;56(6):3496–3504.
14. Scoles D, Gray DC, Hunter JJ, et al. In-vivo imaging of retinal nerve fiber layer vasculature: imaging histology comparison. *BMC Ophthalmol*. 2009;9:9.
15. Nadler Z, Wang B, Schuman JS, et al. In Vivo Three-Dimensional Characterization of the Healthy Human Lamina Cribrosa With Adaptive Optics Spectral-Domain Optical Coherence Tomography. *Invest Ophthalmol Vis Sci*. 2014;55(10):6459–6466.
16. Liu Z, Kurokawa K, Zhang F, Lee JJ, Miller DT. Imaging and quantifying ganglion cells and other transparent neurons in the living human retina. *Proc Natl Acad Sci USA*. 2017;114(48):12803–12808.
17. Liu Z, Saeedi O, Zhang F, et al. Quantification of Retinal Ganglion Cell Morphology in Human Glaucomatous Eyes. *Invest Ophthalmol Vis Sci*. 2021;62(3):34.
18. Soltanian-Zadeh S, Kurokawa K, Liu Z, et al. Weakly supervised individual ganglion cell segmentation from adaptive

optics OCT images for glaucomatous damage assessment. *Optica*. 2021;8(5):642–651.

19. Miller DT, Kurokawa K. Cellular-Scale Imaging of Transparent Retinal Structures and Processes Using Adaptive Optics Optical Coherence Tomography. *Annual Review of Vision Science*. 2020;6(1):115–148.
20. Kurokawa K, Crowell JA, Zhang F, Miller DT. Suite of methods for assessing inner retinal temporal dynamics across spatial and temporal scales in the living human eye. *Neurophotonics*. 2020;7(1):015013.
21. Felberer F, Rechenmacher M, Haindl R, Baumann B, Hitzenberger CK, Pircher M. Imaging of retinal vasculature using adaptive optics SLO/OCT. *Biomed Opt Express*. 2015;6(4):1407–1418.
22. Karst SG, Salas M, Hafner J, et al. Three-Dimensional Analysis of Retinal Microaneurysms with Adaptive Optics Optical Coherence Tomography. *Retina*. 2019;39(3):465–472.
23. Iwasaki M, Inomata H. Relation between superficial capillaries and foveal structures in the human retina. *Invest Ophthalmol Vis Sci*. 1986;27(12):1698–1705.
24. Prum BE, Rosenberg LF, Gedde SJ, et al. Primary Open-Angle Glaucoma Preferred Practice Pattern Guidelines. *Ophthalmology*. 2016;123(1):P41–P111.
25. Hodapp E, Parrish R, Anderson DR. Clinical Decisions In Glaucoma. Published online 1993, https://www.semanticscholar.org/paper/Clinical-Decisions-In-Glaucoma-Hodapp-Parrish/0661773d328bd6c03cf2aaebc648d4264bf98837. Accessed June 22, 2021.
26. Liu Z, Tam J, Saeedi O, Hammer DX. Trans-retinal cellular imaging with multimodal adaptive optics. *Biomed Opt Express, BOE*. 2018;9(9):4246–4262.
27. Curcio CA, Sloan KR. Packing geometry of human cone photoreceptors: variation with eccentricity and evidence for local anisotropy. *Vis Neurosci*. 1992;9(2):169–180.
28. Campbell JP, Zhang M, Hwang TS, et al. Detailed vascular anatomy of the human retina by projection-resolved optical coherence tomography angiography | scientific reports. *Sci Rep*. 2017;7:42201. Accessed June 22, 2021, https://www.nature.com/articles/srep42201.
29. Schindelin J, Arganda-Carreras I, Frise E, et al. Fiji: an open-source platform for biological-image analysis. *Nat Methods*. 2012;9(7):676–682.
30. Tan T-E, Nguyen Q, Chua J, et al. Global Assessment of retinal arteriolar, venular and capillary microcirculations using fundus photographs and optical coherence tomography angiography in diabetic retinopathy. *Sci Rep*. 2019;9(1):11751.
31. An D, Balaratnasingam C, Heisler M, et al. Quantitative comparisons between optical coherence tomography angiography and matched histology in the human eye. *Exper Eye Res*. 2018;170:13–19.
32. SY Yuan, Rigor RR. *Structure and Function of Exchange Microvessels*. Boston, MA: Morgan & Claypool Life Sciences Publishers; 2010, https://www.ncbi.nlm.nih.gov/books/NBK54123/. Accessed June 23, 2021.
33. A general and simple method for obtaining R2 from generalized linear mixed-effects models - Nakagawa - 2013 - Methods in Ecology and Evolution - Wiley Online Library, https://besjournals.onlinelibrary.wiley.com/doi/full/10.1111/j.2041-210x.2012.00261.x. Accessed June 22, 2021.
34. Kim J-S, Kim YK, Baek SU, et al. Topographic correlation between macular superficial microvessel density and ganglion cell-inner plexiform layer thickness in glaucoma-suspect and early normal-tension glaucoma. *Br J Ophthalmol*. 2020;104(1):104–109.
35. Takusagawa HL, Liu L, Ma KN, et al. Projection-Resolved Optical Coherence Tomography Angiography of Macular Retinal Circulation in Glaucoma. *Ophthalmology*. 2017;124(11):1589–1599.
36. Mroczkowska S, Benavente-Perez A, Negi A, Sung V, Patel SR, Gherghel D. Primary Open-Angle Glaucoma vs Normal-Tension Glaucoma: The Vascular Perspective. *JAMA Ophthalmol*. 2013;131(1):36.
37. Baniasadi N, Paschalis EI, Haghzadeh M, et al. Patterns of Retinal Nerve Fiber Layer Loss in Different Subtypes of Open Angle Glaucoma Using Spectral Domain Optical Coherence Tomography. *J Glaucoma*. 2016;25(10):865–872.
38. Jones A, Kaplowitz K, Saeedi O. Autoregulation of optic nerve head blood flow and its role in open-angle glaucoma. *Expert Rev Ophthalmol*. 2014;9(6):487–501.
39. Yu D-Y, Cringle SJ, Yu PK, et al. Retinal capillary perfusion: Spatial and temporal heterogeneity. *Prog Retin Eye Res*. 2019;70:23–54.
40. Dallorto L, Lavia C, Jeannerot A-L, et al. Retinal microvasculature in pituitary adenoma patients: is optical coherence tomography angiography useful? - Dallorto - 2020 - Acta Ophthalmologica - Wiley Online Library, https://onlinelibrary.wiley.com/doi/abs/10.1111/aos.14322. Accessed June 22, 2021.
41. Kisler K, Nelson AR, Montagne A, Zlokovic BV. Cerebral blood flow regulation and neurovascular dysfunction in Alzheimer disease. *Nat Rev Neurosci*. 2017;18(7):419–434.

Investigative Ophthalmology & Visual Science